A Comparison of SNR Estimation Techniques for the AWGN Channel

David R. Pauluzzi and Norman C. Beaulieu, *Fellow, IEEE*

***Abstract*—The performances of several signal-to-noise ratio (SNR) estimation techniques reported in the literature are compared to identify the "best" estimator. The SNR estimators are investigated by the computer simulation of baseband binary phase-shift keying (PSK) signals in real additive white Gaussian noise (AWGN) and baseband 8-PSK signals in complex AWGN. The mean square error is used as a measure of performance. In addition to comparing the relative performances, the absolute levels of performance are also established; the simulated performances are compared to a published Cramér–Rao bound (CRB) for real AWGN and a CRB for complex AWGN that is derived here. Some known estimator structures are modified to perform better on the channel of interest. Estimator structures for both real and complex channels are examined.**

***Index Terms*—Phase-shift keying, signal-to-noise estimation.**

I. Introduction

THE SEARCH for a good signal-to-noise ratio (SNR) estimation technique is motivated by the fact that various algorithms require knowledge of the SNR (see, for example, [1]–[3]) for optimal performance if the SNR is not constant. The performance of diverse systems may be improved if knowledge of the SNR is available. Past engineering practice has often used estimation of the total signal-plus-noise power instead of estimation of the SNR, since it is much easier to measure total power than the ratio of signal power to noise power (or noise power spectral density). However, decreasing hardware costs and increasing demands for pushing system performance to the achievable limits make an investigation of SNR estimation techniques timely.

We compare the performances of various SNR estimation techniques for digital communications channels that have been published in the literature over the last few decades. It is difficult to assess the relative performances of these SNR estimators based on the published results since the performance metrics and the test conditions are not consistent. To make a relevant performance comparison, we implemented each of the estimators in common, simulated channels using a consistent performance metric (the mean square error [MSE]). In order to assess the absolute performances of the estimators, we derive a Cramér–Rao bound (CRB) for complex channels and compare it to a published CRB for real channels. The simulated estimator performances are then compared to CRB's for both the real and complex additive white Gaussian noise (AWGN) channels. To the best of the authors' knowledge, no published study has performed a direct comparison of SNR estimators as provided here. A survey of bit-error rate (BER) estimation techniques was published by Newcombe and Pasupathy [4]. This work did not make quantitative performance comparisons of SNR estimators.

Simulated binary phase-shift keying (PSK) signals in real AWGN and 8-PSK signals in complex AWGN are used to investigate the performances of the various SNR estimators under study. Many of the estimator structures presented here differ in some way from the original published forms since they have been adapted to the system model described in Section II. The published estimators typically are presented either for real channels or complex channels; we extend the published results by providing estimator structures for both cases, where applicable.

The estimators under consideration derive the SNR from the baseband, sampled, data-bearing received signal. The data may either be known (for example, training sequences provided for synchronization and equalization) or unknown to the receiver. Those techniques that derive the SNR estimates solely from the unknown, information-bearing portion of the received signal are known as "in-service" SNR estimators and are of particular interest since they do not impinge upon the throughput of the channel. On the other hand, though SNR estimators using known data can only generate estimates when known data are available, the particular application will dictate whether or not this limitation is objectionable. There is no additional penalty in throughput incurred by using SNR estimators that employ known data in transmission systems that already use training sequences for equalizer or synchronizer training, and these estimators can be expected to perform better. We investigate, therefore, both types of estimators and quantify by example the improvement in performance achievable by using known data rather than error-corrupted recovered data.

Section II provides a statement of the SNR estimation problem and the system model. The various SNR estimators are described in Section III. Performance comparisons and a theoretical limit to performance are reported in Section IV. Section V concludes the paper.

II. System Model

The goal is to find the "best" estimate of the SNR in a digital receiver with the least cost. Generally, SNR estimates are generated by averaging observable properties of the received

Paper approved by R. A. Kennedy, the Editor for Data Communications, Modulation, and Signal Design of the IEEE Communications Society. Manuscript received July 29, 1996; revised May 19, 1998 and November 30, 1999. This work was supported in part by the Telecommunications Research Institute of Ontario (TRIO) and Technology Ontario, Ministry of Economic Development and Trade.

D. R. Pauluzzi is with PMC-Sierra, Inc., Wireless Products Division, Vancouver, BC V6H 3H8, Canada (e-mail: dave_pauluzzi@pmc-sierra.com).

N. C. Beaulieu is with the Department of Electrical and Computer Engineering, Queen's University, Kingston, ON K7L 3N6, Canada (e-mail: beaulieu@ee.queensu.ca).

Publisher Item Identifier S 0090-6778(00)08783-3.

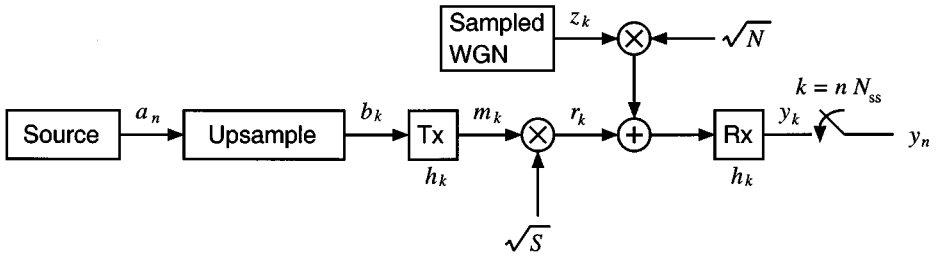

Fig. 1. Baseband-equivalent system model.

signal over a number of symbols. The SNR of interest is the ratio of the discrete signal power to discrete noise power at the input to the decision device at the optimal sampling instants. In the following, "SNR" denotes this ratio of discrete powers. If a matched filter (MF) is employed at the receiver, the SNR ρ as defined here is related to the ratio of the symbol energy-to-noise power spectral density E_s/N_0 by $\rho = 2E_s/N_0$ for real channels and $\rho = E_s/N_0$ for complex channels.

We consider the complex, discrete, baseband-equivalent, band-limited model of coherent M-ary PSK in complex AWGN (which is also a suitable model of binary PSK (BPSK) in real AWGN with minor modifications) illustrated in Fig. 1. Perfect carrier and symbol timing recovery are assumed. A block of N_{sym} M-ary source symbols is upsampled to $N_{\text{ss}} = 16$ samples per symbol, pulse-shaped by a root raised-cosine (RRC) filter (with rolloff $\alpha = 0.5$ and $L = 127$ tap coefficients), scaled by a constant attenuation factor, and corrupted by sampled, complex AWGN. The sequence of M-ary source symbols is represented by

$$a_n = e^{j\theta_n}, \qquad n \in \{0, 1, \ldots, N_{\text{sym}} - 1\} \tag{1}$$

where θ_n is one of M phases spaced evenly around the unit circle. The upsampled M-ary message sequence is given by

$$b_k = \sum_n a_n \delta_{k,\, nN_{\text{ss}}} \tag{2}$$

where δ_{ij} is the Kronecker delta. The sampled, pulse-shaped information signal is given by

$$m_k = \sum_n a_n h_{k-nN_{\text{ss}}} \tag{3}$$

where h_k, $k \in \{-(L-1)/2, \ldots, -1, 0, 1, \ldots, (L-1)/2\}$, represents the RRC filter tap coefficients and $h_k = 0$ for $|k| > (L-1)/2$. The signal presented to the receiver is

$$r_k = \sqrt{S} m_k + \sqrt{N} z_k \tag{4}$$

where z_k is complex, sampled, zero-mean AWGN of unit variance, S is a signal power scale factor, and N is a noise power scale factor. The samples of the received signal after the MF can be expressed as

$$\begin{aligned} y_k &= (\sqrt{S} m_k + \sqrt{N} z_k) \otimes h^*_{-k} \\ &= \sqrt{S} \sum_l h_l m_{k-l} + \sqrt{N} \sum_l h_l z_{k-l} \end{aligned} \tag{5}$$

where $\otimes$ denotes discrete convolution, $*$ denotes complex conjugation, and $h^*_{-k} = h_k$ because the RRC impulse response is assumed to be real and even symmetric. Lastly, the intersymbol interference (ISI)-free output of the MF (the decision variable) is

$$y_n = y_k|_{k=nN_{\text{ss}}} = \sqrt{S} a_n g_0 + \sqrt{N} w_n \tag{6}$$

where g_0 is the peak of the full raised-cosine impulse response whose samples are given by

$$g_k = h_k \otimes h^*_{-k} = \sum_l h_l h_{k-l} \tag{7}$$

and w_n represents the symbol-spaced, filtered noise samples given by

$$w_n = w_k|_{k=nN_{\text{ss}}} = \sum_l h_l z_{k-l} \Big|_{k=nN_{\text{ss}}}. \tag{8}$$

Since y_n is the decision variable, the SNR may be written as

$$\rho = \frac{E\{|\sqrt{S} a_n g_0|^2\}}{\text{var}\{\sqrt{N} w_n\}} \tag{9}$$

where $E\{\cdot\}$ and $\text{var}\{\cdot\}$ denote expectation and variance, respectively. Setting the sum of the squares of the RRC tap coefficients to unity makes the SNR independent of the channel; it may then be set solely by the appropriate selection of S and N so that $\rho = S/N$.

III. SNR Estimators

Estimators that rely on knowledge of the transmitted data are designated as *data-aided* (DA). A DA estimator that makes use of perfect knowledge of the transmitted sequence is denoted by *TxDA*. A DA estimator that uses an *estimate* of the transmitted data sequence from receiver decisions is denoted by *RxDA*. Where applicable, estimator expressions are provided for both real and complex channels.

A. Split-Symbol Moments Estimator (SSME)

The original formulation of the SSME algorithm by Simon and Mileant assumes BPSK modulation in a wide-band AWGN channel [5]. This estimator is designated SSME_0. Shah and Hinedi [6] investigated the performance of the SSME_0 in band-limited channels, and further work by Shah and Holmes [7] was aimed at improving the performance of the SSME_0 in narrow-band channels where the system impulse response is known or can be measured. The general approach of Shah and Holmes is outlined below, where adaption of their algorithm

to the system model described in Section II gives an estimator which we designate as SSME_1.

The SNR is found as the ratio of S to N where S and N are the solutions to the system of linear equations given by

$$\begin{aligned} m_{\text{p}} &= c_{11}S + c_{12}N \\ m_{\text{ss}} &= c_{21}S + c_{22}N. \end{aligned} \tag{10}$$

The quantities m_{p} and m_{ss} are computed as

$$m_{\text{p}} = \frac{1}{N_{\text{sym}}} \sum_{n=0}^{N_{\text{sym}}-1} Y_{\alpha n} Y_{\beta n} \tag{11}$$

and

$$m_{\text{ss}} = \frac{1}{N_{\text{sym}}} \sum_{n=0}^{N_{\text{sym}}-1} (Y_{\alpha n} + Y_{\beta n})^2 \tag{12}$$

where $Y_{\alpha n}$ and $Y_{\beta n}$ are obtained from y_k in (5) by setting

$$Y_{\alpha n} = \sum_{k=nN_{\text{ss}}}^{nN_{\text{ss}}+N_{\text{ss}}/2-1} y_k \tag{13}$$

and

$$Y_{\beta n} = \sum_{k=nN_{\text{ss}}+N_{\text{ss}}/2}^{(n+1)N_{\text{ss}}-1} y_k. \tag{14}$$

The coefficients c_{ij} may be found by taking the expected values of m_{p} and m_{ss} in (11) and (12), respectively, and are functions of the transmitter and receiver filter coefficients.

We have also examined a variation of the SSME method that results from the replacement of m_{p} and m_{ss} with m_{q} and m_{sq} where

$$\begin{aligned} m_{\text{q}} = &\left(\frac{1}{N_{\text{sym}}} \sum_{n_1=0}^{N_{\text{sym}}-1} \sum_{k_1=n_1N_{\text{ss}}}^{n_1N_{\text{ss}}+N_{\text{ss}}/2-1} y_{k_1}^2 \right) \\ &\cdot \left(\frac{1}{N_{\text{sym}}} \sum_{n_2=0}^{N_{\text{sym}}-1} \sum_{k_2=n_2N_{\text{ss}}+N_{\text{ss}}/2}^{(n_2+1)N_{\text{ss}}-1} y_{k_2}^2 \right) \end{aligned} \tag{15}$$

and

$$m_{\text{sq}} = \frac{1}{N_{\text{sym}}N_{\text{ss}}} \sum_{n=0}^{N_{\text{sym}}-1} \sum_{k=nN_{\text{ss}}}^{(n+1)N_{\text{ss}}-1} y_k^4. \tag{16}$$

The SNR is again found as the ratio of S to N, but in this case, S and N are the solutions to the system of quadratic equations given by

$$\begin{aligned} m_{\text{q}} &= d_{11}S^2 + d_{12}SN + d_{13}N^2 \\ m_{\text{sq}} &= d_{21}S^2 + d_{22}SN + d_{23}N^2. \end{aligned} \tag{17}$$

The coefficients d_{ij} may be found by taking the expected values of m_{q} and m_{sq} in (15) and (16), respectively. Like the c_{ij}, the d_{ij} are dependent on the impulse response of the system. The lengthy expressions for c_{ij} and d_{ij} are omitted but may be found in [8]. This variation of the SSME method was originated by the authors in an attempt to improve the performance of the SSME_1 for narrow-band channels. We designate this estimator SSME_2.

All of the SSME methods (SSME_0, SSME_1, and SSME_2) are examples of in-service estimators, and they may only be applied to BPSK-modulated signals in real AWGN. Complex forms of the SSME algorithms are not presented since none of these methods is easily extended to higher orders of modulation. The SSME algorithms are the only SNR estimators considered here for which complex forms are not provided.

B. Maximum-Likelihood (ML) Estimator for SNR

This SNR estimator, based on ML estimation theory [9], was introduced by Kerr [10] and Gagliardi and Thomas [11]. The latter treatment is more detailed. Gagliardi and Thomas derived and studied the ML SNR estimator for a BPSK-modulated signal in real AWGN. We extend the application of this estimator below to M-ary PSK signals in complex AWGN.

The ML estimator is derived from samples of the complex received signal given by (4), which may be rewritten explicitly in terms of real and imaginary parts as

$$r_k = r_{I_k} + jr_{Q_k} = \sqrt{S}(m_{I_k} + jm_{Q_k}) + \sqrt{N}(z_{I_k} + jz_{Q_k}). \tag{18}$$

Let $\nu_{I_k} = \sqrt{N}z_{I_k}$ and $\nu_{Q_k} = \sqrt{N}z_{Q_k}$ represent the in-phase and quadrature components of the noise, respectively, each having zero mean and variance $N/2$. Assuming the in-phase and quadrature components of the noise are independent, their joint probability density function (pdf) is

$$f(\nu_{I_k}, \nu_{Q_k}) = \frac{1}{\pi N} e^{-(\nu_{I_k}^2 + \nu_{Q_k}^2)/N}. \tag{19}$$

Using (18) and (19), the joint pdf of the in-phase and quadrature components of a received signal sample may be written as

$$\begin{aligned} &f(r_{I_k}, r_{Q_k}|S, N, i) \\ &\quad = \frac{1}{\pi N} \exp\left(-\frac{\left(r_{I_k} - \sqrt{S}m_{I_k}^{(i)}\right)^2 + \left(r_{Q_k} - \sqrt{S}m_{Q_k}^{(i)}\right)^2}{N} \right) \end{aligned} \tag{20}$$

where $m_{I_k}^{(i)}$ and $m_{Q_k}^{(i)}$ are the real and imaginary parts of (3), respectively, and the superscript i denotes the ith sequence of $M^{N_{\text{sym}}}$ possible transmitted message sequences. Both the signal and noise sequences are assumed independent so that the joint pdf of the $K = N_{\text{sym}}N_{\text{ss}}$ received samples is given by

$$\begin{aligned} &f(\mathbf{r_I}, \mathbf{r_Q}|S, N, i) \\ &\quad = \prod_{k=0}^{K-1} f(r_{I_k}, r_{Q_k}|S, N, i) \\ &\quad = (\pi N)^{-K} \exp\left[-\frac{1}{N} \left(\sum_{k=0}^{K-1} \left(r_{I_k} - \sqrt{S}m_{I_k}^{(i)} \right)^2 \right.\right. \\ &\qquad \left.\left. + \sum_{k=0}^{K-1} \left(r_{Q_k} - \sqrt{S}m_{Q_k}^{(i)} \right)^2 \right) \right] \end{aligned} \tag{21}$$

where $\mathbf{r_I}$ is the sequence $\{r_{I_0}, r_{I_1}, \ldots, r_{I_{K-1}}\}$ and $\mathbf{r_Q}$ is the sequence $\{r_{Q_0}, r_{Q_1}, \ldots, r_{Q_{K-1}}\}$. The likelihood function $\Gamma(S, N, i)$ is

$$\begin{aligned}\Gamma(S, N, i) &= \ln f(\mathbf{r_I}, \mathbf{r_Q}|S, N, i) \\ &= -K \ln(\pi N) - \frac{1}{N} \\ &\quad \cdot \left[\sum_{k=0}^{K-1} \left(r_{I_k} - \sqrt{S} m_{I_k}^{(i)}\right)^2 + \sum_{k=0}^{K-1} \left(r_{Q_k} - \sqrt{S} m_{Q_k}^{(i)}\right)^2\right].\end{aligned} \tag{22}$$

To find the ML estimate of the SNR $\hat{\rho}_{\mathrm{ML}}$, we use the property that the ML estimate of the ratio of two parameters (in this case, S and N) is the ratio of the individual ML estimates of the two parameters [11]. This convenient property allows the ML SNR estimator to be written as

$$\hat{\rho}_{\mathrm{ML}} = \frac{\hat{S}_{\mathrm{ML}}}{\hat{N}_{\mathrm{ML}}} \tag{23}$$

and all that is necessary is to find $\hat{S}_{\mathrm{ML}}$ and $\hat{N}_{\mathrm{ML}}$ as the solution of the system of equations

$$\begin{aligned}\left.\frac{\partial}{\partial S}\Gamma(S, N, i)\right|_{\substack{S=\hat{S}_{\mathrm{ML}} \\ N=\hat{N}_{\mathrm{ML}} \\ i=\hat{i}_{\mathrm{ML}}}} &= 0 \\ \left.\frac{\partial}{\partial N}\Gamma(S, N, i)\right|_{\substack{S=\hat{S}_{\mathrm{ML}} \\ N=\hat{N}_{\mathrm{ML}} \\ i=\hat{i}_{\mathrm{ML}}}} &= 0.\end{aligned} \tag{24}$$

The respective solutions for $\hat{S}_{\mathrm{ML}}$ and $\hat{N}_{\mathrm{ML}}$ are written as

$$\hat{S}_{\mathrm{ML}} = \left[\frac{\frac{1}{K}\sum_{k=0}^{K-1}\left(r_{I_k} m_{I_k}^{(i)} + r_{Q_k} m_{Q_k}^{(i)}\right)}{\frac{1}{K}\sum_{k=0}^{K-1}\left[\left(m_{I_k}^{(i)}\right)^2 + \left(m_{Q_k}^{(i)}\right)^2\right]}\right]^2 \tag{25}$$

and

$$\begin{aligned}\hat{N}_{\mathrm{ML}} &= \frac{1}{K}\sum_{k=0}^{K-1}\left(r_{I_k}^2 + r_{Q_k}^2\right) \\ &\quad -\hat{S}\frac{1}{K}\sum_{k=0}^{K-1}\left[\left(m_{I_k}^{(i)}\right)^2 + \left(m_{Q_k}^{(i)}\right)^2\right].\end{aligned} \tag{26}$$

Given the system model of Section II, $E\{(1/K)\sum_k (m_{I_k}^{(i)})^2 + (m_{Q_k}^{(i)})^2\} = g_0 \mathrm{var}\{a_n\}/N_{\mathrm{ss}} = 1/N_{\mathrm{ss}}$ so that an in-service, ML RxDA SNR estimator for complex signals may be written compactly as

$$\begin{aligned}\hat{\rho}_{\mathrm{ML\ RxDA,\,complex}} &= \frac{\hat{S}_{\mathrm{ML}}}{\hat{N}_{\mathrm{ML}}} \\ &= \frac{N_{\mathrm{ss}}^2\left[\frac{1}{K}\sum_{k=0}^{K-1}\mathrm{Re}\left\{r_k^* m_k^{(i)}\right\}\right]^2}{\frac{1}{K}\sum_{k=0}^{K-1}|r_k|^2 - N_{\mathrm{ss}}\left[\frac{1}{K}\sum_{k=0}^{K-1}\mathrm{Re}\left\{r_k^* m_k^{(i)}\right\}\right]^2}\end{aligned} \tag{27}$$

where $\mathrm{Re}\{\cdot\}$ denotes the real part of a complex quantity. The ML SNR estimator for real channels is obtained by replacing complex quantities in (27) with corresponding real ones.

For the real case, Thomas [12] derived the pdf of the ML SNR estimator and used it to show that the estimator has a bias which may be reduced by multiplying the denominator of the ML expression by $K/(K-3)$. Replacing complex quantities with real ones in (27), and applying this factor to the denominator, a reduced-bias, in-service, ML SNR estimator for real channels may be written as

$$\begin{aligned}\hat{\rho}'_{\mathrm{ML\ RxDA,\,real}} &= \frac{N_{\mathrm{ss}}^2\left[\frac{1}{K}\sum_{k=0}^{K-1} r_k m_k^{(i)}\right]^2}{\frac{1}{K-3}\sum_{k=0}^{K-1} r_k^2 - \frac{N_{\mathrm{ss}}}{K(K-3)}\left[\sum_{k=0}^{K-1} r_k m_k^{(i)}\right]^2}\end{aligned} \tag{28}$$

where $\hat{\rho}'$ is used to denote a reduced-bias estimator. For complex channels, a reduced-bias, in-service, ML RxDA SNR estimator may be derived to obtain

$$\begin{aligned}\hat{\rho}'_{\mathrm{ML\ RxDA,\,complex}} &= \frac{N_{\mathrm{ss}}^2\left[\frac{1}{K}\sum_{k=0}^{K-1}\mathrm{Re}\left\{r_k^* m_k^{(i)}\right\}\right]^2}{\frac{1}{K-3/2}\sum_{k=0}^{K-1}|r_k|^2 - \frac{N_{\mathrm{ss}}}{K(K-3/2)}\left[\sum_{k=0}^{K-1}\mathrm{Re}\left\{r_k^* m_k^{(i)}\right\}\right]^2}.\end{aligned} \tag{29}$$

This result holds because the number of degrees of freedom in the denominator in the complex case is twice that of the real case. Equation (29) may be used in systems where coherent M-ary PSK modulation is employed in a complex AWGN channel, and it is easily extended to other coherent digital modulation schemes, such as QAM. Both (28) and (29) are in-service, RxDA estimators since the pulse-shaped samples $m_k^{(i)}$ are based on receiver decisions. Replacing the estimated, pulse-shaped samples with the exact, pulse-shaped, transmitted samples m_k yields the TxDA forms of the ML estimators (which, of course, are not of the in-service type).

The ML RxDA and ML TxDA SNR estimators, and the SSME series of SNR estimators discussed in the previous section, are the only estimator structures in this paper that operate with more than one sample per symbol. The remaining techniques discussed in Section III-C–III-E operate on the one optimal sample per symbol at the output of the MF.

C. Squared Signal-to-Noise Variance (SNV) Estimator

This in-service RxDA SNR estimator is based on the first absolute moment and the second moment of the sampled output of the MF. It was first introduced by Gilchriest in 1966 for BPSK signals in real AWGN [13]. We first present the original formulation of the SNV RxDA estimator for BPSK modulation in real AWGN, and then suggest how the bias of the original version may be reduced. A reduced-bias TxDA form of the SNV estimator is presented for real channels, and finally, we extend the scope of the SNV estimators from BPSK modulation in real channels to higher orders of modulation in complex channels.

The SNV RxDA estimator, as given in [13] for BPSK in real AWGN, is expressed in terms of the sampled output of the MF as

$$\hat{\rho}_{\text{SNV RxDA, real}} = \frac{\left[\dfrac{1}{N_{\text{sym}}}\displaystyle\sum_{n=0}^{N_{\text{sym}}-1}|y_n|\right]^2}{\dfrac{1}{N_{\text{sym}}-1}\displaystyle\sum_{n=0}^{N_{\text{sym}}-1}y_n^2-\dfrac{1}{N_{\text{sym}}(N_{\text{sym}}-1)}\left[\displaystyle\sum_{n=0}^{N_{\text{sym}}-1}|y_n|\right]^2} \tag{30}$$

which is remarkably similar in form to (28) with $N_{\text{ss}}=1$. In fact, the factor $1/(N_{\text{sym}}-1)$ in the denominator of (30) may be replaced with the factor $1/(N_{\text{sym}}-3)$ to produce a reduced-bias estimator for real channels as was done for the ML estimators for real channels described in the previous section.

The SNV SNR estimator is actually a special case of the ML SNR estimator. Whereas the ML SNR estimator operates on N_{ss} samples per symbol at the input to the MF, the SNV SNR estimator operates on the optimally sampled output of the MF. The ML SNR algorithm may be applied at that point since the symbol-spaced, filtered noise samples are white (assuming a root-Nyquist filter is employed in the receiver).

An SNV TxDA SNR estimator may be written as a modification of (30) by recognizing that $|y_n| = y_n a_n^{(i)}$, where i denotes the ith sequence of $2^{N_{\text{sym}}}$ possible sequences, and $\hat{\imath}$ represents the sequence of symbols estimated by the receiver. This relation holds true because a_n, as given by (1), is either 1 or -1 for BPSK signals in real channels. A TxDA form is obtained by replacing the estimated symbols $a_n^{(i)}$ with the known transmitted symbols a_n to yield the reduced-bias, SNV TxDA SNR estimator for real channels as

$$\hat{\rho}'_{\text{SNV TxDA, real}} = \frac{\left[\dfrac{1}{N_{\text{sym}}}\displaystyle\sum_{n=0}^{N_{\text{sym}}-1}y_n a_n\right]^2}{\dfrac{1}{N_{\text{sym}}-3}\displaystyle\sum_{n=0}^{N_{\text{sym}}-1}y_n^2-\dfrac{1}{N_{\text{sym}}(N_{\text{sym}}-3)}\left[\displaystyle\sum_{n=0}^{N_{\text{sym}}-1}y_n a_n\right]^2}. \tag{31}$$

Since the SNV estimator is a special case of the ML SNR estimator, the reduced-bias form of the *complex*, in-service, SNV RxDA estimator may be expressed as an appropriate adaptation of (29) as shown in (32), at the bottom of the page, where $a_n^{(i)}$ was identified above as the receiver estimates of the transmitted symbols (which, in this case, are complex-valued). The SNV TxDA estimator for complex channels is obtained simply by the substitution of the receiver estimates $a_n^{(i)}$ with the known, unfiltered source symbols a_n in a similar manner as described above for the real case. The estimator given by (32) and its TxDA counterpart are applicable to M-ary PSK and are easily extended to other coherent modulation schemes such as QAM.

D. Second- and Fourth-Order Moments (M_2M_4) Estimator

An early mention of the application of second- and fourth-order moments to the separate estimation of carrier strength and noise strength in real AWGN channels was in 1967 by Benedict and Soong [14]. In 1993, Matzner [15] gave a detailed derivation of an SNR estimator which yielded similar expressions to those given in [14]. In 1994, Matzner and Engleberger [16] rederived the estimator for real signals using a different approach. We sketch the derivation provided in [15] for complex channels below, and then show how the estimator can be modified for application to real channels using the same approach.

Let M_2 denote the second moment of y_n as

$$\begin{aligned} M_2 &= E\{y_n y_n^*\} \\ &= SE\{|a_n|^2\} + \sqrt{SN}E\{a_n w_n^*\} \\ &\quad + \sqrt{SN}E\{a_n^* w_n\} + NE\{|w_n|^2\} \end{aligned} \tag{33}$$

$$\hat{\rho}'_{\text{SNV RxDA, complex}} = \frac{\left[\dfrac{1}{N_{\text{sym}}}\displaystyle\sum_{n=0}^{N_{\text{sym}}-1}\text{Re}\left\{y_n^* a_n^{(i)}\right\}\right]^2}{\dfrac{1}{N_{\text{sym}}-3/2}\displaystyle\sum_{n=0}^{N_{\text{sym}}-1}|y_n|^2-\dfrac{1}{N_{\text{sym}}(N_{\text{sym}}-3/2)}\left[\displaystyle\sum_{n=0}^{N_{\text{sym}}-1}\text{Re}\left\{y_n^* a_n^{(i)}\right\}\right]^2} \tag{32}$$

and let M_4 denote the fourth moment of y_n as

$$\begin{aligned} M_4 &= E\{(y_n y_n^*)^2\} \\ &= S^2 E\{|a_n|^4\} + 2S\sqrt{SN} \\ &\quad \cdot (E\{|a_n|^2 a_n w_n^*\} + E\{|a_n|^2 a_n^* w_n\}) + SN \\ &\quad \cdot (E\{(a_n w_n^*)^2\} + 4E\{|a_n|^2 |w_n|^2\} + E\{(a_n^* w_n)^2\}) \\ &\quad + 2N\sqrt{SN}(E\{|w_n|^2 a_n w_n^*\} + E\{|w_n|^2 a_n^* w_n\}) \\ &\quad + N^2 E\{|w_n|^4\}. \end{aligned} \tag{34}$$

Assuming the signal and noise are zero-mean, independent random processes, and the in-phase and quadrature components of the noise are independent, (33) and (34) reduce to

$$M_2 = S + N \tag{35}$$

and

$$M_4 = k_a S^2 + 4SN + k_w N^2 \tag{36}$$

respectively, where $k_a = E\{|a_n|^4\}/E\{|a_n|^2\}^2$ and $k_w = E\{|w_n|^4\}/E\{|w_n|^2\}^2$ are the kurtosis of the signal and the kurtosis of the noise, respectively. Solving for S and N, one obtains

$$\hat{S} = \frac{M_2(k_w - 2) \pm \sqrt{(4 - k_a k_w){M_2}^2 + M_4(k_a + k_w - 4)}}{k_a + k_w - 4} \tag{37}$$

and

$$\hat{N} = M_2 - \hat{S}. \tag{38}$$

The estimator formed as the ratio of $\hat{S}$ to $\hat{N}$ is denoted the M_2M_4 estimator. As an example, for any M-ary PSK signal, $k_a = 1$, and for complex noise, $k_w = 2$, so that

$$\hat{\rho}_{M_2M_4,\,\text{complex}} = \frac{\sqrt{2{M_2}^2 - M_4}}{M_2 - \sqrt{2{M_2}^2 - M_4}} \tag{39}$$

where the negative root in (37) is selected so that $\hat{\rho}_{M_2M_4,\,\text{complex}}$ is positive. In a similar manner, assuming y_n is real, $M_2 = E\{y_n^2\}$ is equivalent to (35), but $M_4 = E\{y_n^4\}$ is given by

$$M_4 = k_a S^2 + 6SN + k_w N^2. \tag{40}$$

Solving (35) and (40) for N gives the same expression as (38), but the solution for S is

$$\hat{S} = \frac{M_2(k_w - 3) \pm \sqrt{(9 - k_a k_w){M_2}^2 + M_4(k_a + k_w - 6)}}{k_a + k_w - 6}. \tag{41}$$

As an example, for BPSK signals, $k_a = 1$, and for real noise, $k_w = 3$, so that

$$\hat{\rho}_{M_2M_4,\,\text{real}} = \frac{\frac{1}{2}\sqrt{6{M_2}^2 - 2M_4}}{M_2 - \frac{1}{2}\sqrt{6M_2^2 - 2M_4}} \tag{42}$$

where, again, the negative root in the expression for $\hat{S}$ is chosen so that $\hat{\rho}_{M_2M_4,\,\text{real}}$ is positive. The M_2M_4 estimator is of the in-service type, and has the advantage that carrier phase recovery is not required since it is based on the second and fourth moments of the signal. As a moments-based estimator, it does not use receiver decisions and so is not labeled as a DA estimator. In practice, the second and fourth moments are estimated by their respective time averages for both real and complex channels as

$$M_2 \approx \frac{1}{N_{\text{sym}}} \sum_{n=0}^{N_{\text{sym}}-1} |y_n|^2 \tag{43}$$

and

$$M_4 \approx \frac{1}{N_{\text{sym}}} \sum_{n=0}^{N_{\text{sym}}-1} |y_n|^4. \tag{44}$$

E. Signal-to-Variation Ratio (SVR) Estimator

The signal-to-variation ratio (SVR) estimator, described by Brandão *et al.* in [17], is a moments-based method developed for monitoring channel quality in multipath fading channels, but it can also be applied as a measure of channel quality in an AWGN channel. This estimator was designed to operate on any M-ary PSK-modulated signal, but it is not applicable, in general, to other digital modulation schemes. We sketch, below, the derivation of the in-service SVR estimator for complex channels based on a development similar to that given in [17]. We then show how the estimator can be modified for application to real channels.

The SVR estimator is a function of the parameter

$$\beta = \frac{E\{y_n y_n^* y_{n-1} y_{n-1}^*\}}{E\{(y_n y_n^*)^2\} - E\{y_n y_n^* y_{n-1} y_{n-1}^*\}}. \tag{45}$$

The term $E\{(y_n y_n^*)^2\}$ is M_4 of the M_2M_4 method of Section III-D given by (36). The other term in (45) simplifies to

$$E\{y_n y_n^* y_{n-1} y_{n-1}^*\} = S^2 + 2SN + N^2 \tag{46}$$

taking advantage of the independence of the signal and noise samples. Writing S/N as ρ, and substituting (36) and (46) into (45), the result is

$$\beta = \frac{\rho^2 + 2\rho + 1}{(k_a - 1)\rho^2 + 2\rho + (k_w - 1)} \tag{47}$$

which may be solved for ρ to yield the general SVR estimator for complex channels as

$$\hat{\rho}_{\text{SVR, complex}} = \frac{(\beta - 1) \pm \sqrt{(\beta-1)^2 - [1 - \beta(k_a - 1)][1 - \beta(k_w - 1)]}}{1 - \beta(k_a - 1)}. \tag{48}$$

As indicated in Section III-D, for M-ary PSK signals in complex AWGN, $k_a = 1$ and $k_w = 2$ so that, taking the positive root, (48) simplifies to

$$\hat{\rho}_{\text{SVR, complex}} = \beta - 1 + \sqrt{\beta(\beta - 1)}. \tag{49}$$

For real signals

$$\beta = \frac{E\{y_n^2 y_{n-1}^2\}}{E\{y_n^4\} - E\{y_n^2 y_{n-1}^2\}} \tag{50}$$

where $E\{y_n^4\}$ is given by (40), and $E\{y_n^2 y_{n-1}^2\}$ simplifies to the same expression as (46). Substituting (40) and (46) into (50), the general SVR estimator for real channels is

$$\hat{\rho}_{\mathrm{SVR,\,real}} = \frac{(2\beta-1) \pm \sqrt{(2\beta-1)^2-[1-\beta(k_a-1)][1-\beta(k_w-1)]}}{1-\beta(k_a-1)}. \tag{51}$$

For a BPSK-modulated signal in real AWGN, $k_a = 1$ and $k_w = 3$ so that, taking the positive root, (51) simplifies to

$$\hat{\rho}_{\mathrm{SVR,\,real}} = (2\beta-1) + \sqrt{2\beta(2\beta-1)}. \tag{52}$$

In practice, the parameter β is estimated by its corresponding time average as

$$\beta = \frac{\dfrac{1}{N_{\mathrm{sym}}-1}\displaystyle\sum_{n=1}^{N_{\mathrm{sym}}-1} |y_n|^2|y_{n-1}|^2}{\dfrac{1}{N_{\mathrm{sym}}-1}\displaystyle\sum_{n=1}^{N_{\mathrm{sym}}-1} |y_n|^4 - \dfrac{1}{N_{\mathrm{sym}}-1}\displaystyle\sum_{n=1}^{N_{\mathrm{sym}}-1} |y_n|^2|y_{n-1}|^2} \tag{53}$$

which, as written, applies to both real and complex channels. Note that recovery of carrier phase is not required for this method since the phase information is removed in the estimation process.

IV. Performance Comparisons

The "best" SNR estimator is the one that is unbiased (or exhibits the smallest bias) and has the smallest variance. The statistical MSE reflects both the bias and the variance of an SNR estimate and is given by

$$\mathrm{MSE}\{\hat{\rho}\} = E\{(\hat{\rho}-\rho)^2\} \tag{54}$$

where $\hat{\rho}$ is an estimate of the SNR, and ρ is the true SNR. We have computed the sample MSE for each estimator by simulation from a number of estimates $\hat{\rho}_i$ according to

$$\mathrm{MSE}\{\hat{\rho}\} = \frac{1}{N_t}\sum_{i=1}^{N_t}(\hat{\rho}_i-\rho)^2. \tag{55}$$

The number of trials N_t was chosen large enough in all cases to ensure an error of less than 20% with 95% confidence.

A. CRB

In order to assess the absolute performance of each estimator, the CRB is used as a reference. Thomas [12] derives the CRB for real channels. Based on [9] and [12], we extend the derivation to complex channels below and compare the result to the real case.

Consider a random variable x whose value (in general complex) is dependent on a vector $\boldsymbol{\theta} = \{\theta_1, \theta_2\}$, where θ_1 and θ_2 are two real, unknown parameters. Assume K such observations of x are available to form the observation vector $\mathbf{x} = \{x_0, x_1, \ldots, x_{K-1}\}$. The objective is to find a lower bound on the variance of any estimator $\hat{\boldsymbol{\theta}}(\mathbf{x})$, which generates estimates of $\boldsymbol{\theta}$ based on the observations $\mathbf{x}$. Following the discussions of the CRB in [9] and [12], we obtain

$$\mathrm{var}\{\hat{\rho}\} \geq \frac{-\left(\dfrac{\partial}{\partial\rho}E\{\hat{\rho}\}\right)^2 E\left\{\dfrac{\partial^2\Gamma}{\partial N^2}\right\}}{E\left\{\dfrac{\partial^2\Gamma}{\partial\rho^2}\right\}E\left\{\dfrac{\partial^2\Gamma}{\partial N^2}\right\} - E\left\{\dfrac{\partial^2\Gamma}{\partial\rho\partial N}\right\}^2}. \tag{56}$$

Rewriting $\Gamma(S, N, i)$ of (22) in terms of ρ and N, the result is

$$\begin{aligned}\Gamma(\rho, N, i) &= \ln f(\mathbf{r_I}, \mathbf{r_Q}|\rho, N, i)\\ &= -K\ln(\pi N) - \frac{1}{N}\\ &\quad\cdot\left[\sum_{k=0}^{K-1}\left(r_{I_k} - \sqrt{\rho N}m_{I_k}^{(i)}\right)^2\right.\\ &\quad\left.+\sum_{k=0}^{K-1}\left(r_{Q_k} - \sqrt{\rho N}m_{Q_k}^{(i)}\right)^2\right].\end{aligned} \tag{57}$$

The required partial derivatives of (57) are

$$\frac{\partial^2\Gamma}{\partial\rho^2} = -\frac{1}{2\sqrt{\rho^3 N}}\sum_{k=0}^{K-1}\left(r_{I_k}m_{I_k}^{(i)} + r_{Q_k}m_{Q_k}^{(i)}\right) \tag{58}$$

$$\begin{aligned}\frac{\partial^2\Gamma}{\partial N^2} &= \frac{K}{N^2} - \frac{2}{N^3}\sum_{k=0}^{K-1}(r_{I_k}^2 + r_{Q_k}^2)\\ &\quad+\frac{3}{2}\sqrt{\frac{\rho}{N^5}}\sum_{k=0}^{K-1}\left(r_{I_k}m_{I_k}^{(i)} + r_{Q_k}m_{Q_k}^{(i)}\right)\end{aligned} \tag{59}$$

$$\frac{\partial^2\Gamma}{\partial\rho\partial N} = -\frac{1}{2\sqrt{\rho N^3}}\sum_{k=0}^{K-1}\left(r_{I_k}m_{I_k}^{(i)} + r_{Q_k}m_{Q_k}^{(i)}\right). \tag{60}$$

The corresponding expected values of the partial derivatives are

$$E\left\{\frac{\partial^2\Gamma}{\partial\rho^2}\right\} = -\frac{K}{2\rho N_{\mathrm{ss}}} \tag{61}$$

$$E\left\{\frac{\partial^2\Gamma}{\partial N^2}\right\} = -\frac{K(2+\rho/N_{\mathrm{ss}})}{2N^2} \tag{62}$$

$$E\left\{\frac{\partial^2\Gamma}{\partial\rho\partial N}\right\} = -\frac{K}{2NN_{\mathrm{ss}}}. \tag{63}$$

Substituting these expressions into (56), recalling that $K = N_{\mathrm{ss}}N_{\mathrm{sym}}$, and assuming $\hat{\rho}$ is unbiased, one obtains the CRB for unbiased SNR estimators in complex AWGN channels as

$$\mathrm{var}\{\hat{\rho}\} \geq \frac{2\rho}{N_{\mathrm{sym}}} + \frac{\rho^2}{N_{\mathrm{ss}}N_{\mathrm{sym}}}. \tag{64}$$

Normalization by ρ^2 shows explicitly the asymptotic behavior of the estimators with increasing SNR; therefore, our results are presented in terms of the normalized MSE (NMSE)

$$\mathrm{NMSE}\{\hat{\rho}\} = \frac{\mathrm{MSE}\{\hat{\rho}\}}{\rho^2} = \frac{\mathrm{var}\{\hat{\rho}\}}{\rho^2} \geq \frac{2}{\rho N_{\mathrm{sym}}} + \frac{1}{N_{\mathrm{ss}}N_{\mathrm{sym}}} \tag{65}$$

where $\mathrm{MSE}\{\hat{\rho}\} = \mathrm{var}\{\hat{\rho}\}$ because $\hat{\rho}$ is assumed unbiased. For real channels, the likelihood function is

$$\Gamma(\rho, N, i) = -\frac{K}{2}\ln(2\pi N) - \frac{1}{2N}\sum_{k=0}^{K-1}\left(r_k - \sqrt{\rho N}m_k^{(i)}\right)^2 \tag{66}$$

so, after taking expected values of partial derivatives, substituting into (56), and assuming an unbiased estimator, the CRB for unbiased SNR estimators in real channels may be expressed in terms of the normalized MSE as

$$\mathrm{NMSE}\{\hat{\rho}\} \geq 2\left(\frac{2}{\rho N_{\mathrm{sym}}} + \frac{1}{N_{\mathrm{ss}}N_{\mathrm{sym}}}\right). \tag{67}$$

Note that the lower bound on SNR estimator variance is a factor of two smaller for complex channels as compared to that for real channels.

B. Simulation Results

The estimators are compared graphically by plotting the NMSE of each estimator for BPSK- and 8-PSK-modulated signals operating in the channel model described in Section II. The appropriate CRB for unbiased estimators is shown for reference, using (67) for BPSK signals and (65) for 8-PSK signals. Note that the CRB for unbiased estimators is not specific to any particular biased estimator.

For ML estimators, which operate on samples at the input to the MF, the constants to be used in (65) and (67) are $N_{\mathrm{ss}} = 16$ and $N_{\mathrm{sym}} = 1024$ or 64. We denote this particular form of the CRB as the *pre-MF CRB*. The SSME_1 and SSME_2 operate on the $N_{\mathrm{ss}} = 16$ samples per symbol at the MF output so a different CRB which takes into account the correlation of the noise samples applies. Though this more complicated CRB indicates how closely the performances of the SSME_1 and SSME_2 approach a theoretical bound for SNR estimators operating on correlated samples, it is more interesting to compare the performances of the SSME_1 and SSME_2 to the pre-MF CRB and the ML results. Therefore, the CRB applicable to the correlated samples at the output of the MF is not considered.

The other estimators under study operate at the output of the MF on the *one* sample per symbol from which receiver decisions are derived. The filtered noise corrupting these samples is uncorrelated since an RRC filter is employed in the receiver, so the CRB developed in Section IV-A applies. For this case, the constants to be used in (65) and (67) are $N_{\mathrm{ss}} = 1$ and $N_{\mathrm{sym}} = 1024$ or 64. We denote this particular form of the CRB as the *post-MF CRB*.

Plots of the normalized sample bias of the estimators, computed from N_t trials as

$$\frac{\mathrm{Bias}\{\hat{\rho}\}}{\rho} = \frac{1}{N_t}\sum_{i=1}^{N_t}\frac{\hat{\rho}_i - \rho}{\rho} \tag{68}$$

accompany some of the NMSE plots in order to identify the degree to which the bias affects the NMSE.

Figs. 2–4 compare the performances of the SSME_1, SSME_2, ML TxDA, and ML RxDA SNR estimators for BPSK-modulated signals in a real AWGN channel. In Fig. 2, $N_{\mathrm{sym}} = 1024$ symbols and $N_{\mathrm{ss}} = 16$ samples per symbol are used to generate an SNR estimate. Results for $N_{\mathrm{sym}} = 64$ symbols are given in Fig. 4 where the curves for the SSME_1 and SSME_2 are omitted since these estimators perform poorly using this smaller number of symbols. Accompanying Fig. 2, Fig. 3 shows the estimator biases using a block length of 1024 symbols.

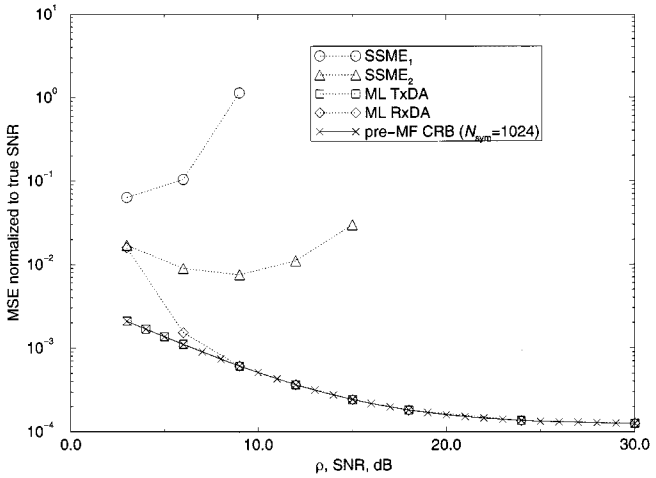

Fig. 2. Normalized MSE with BPSK signals in real AWGN ($N_{\mathrm{ss}} = 16$ and $N_{\mathrm{sym}} = 1024$).

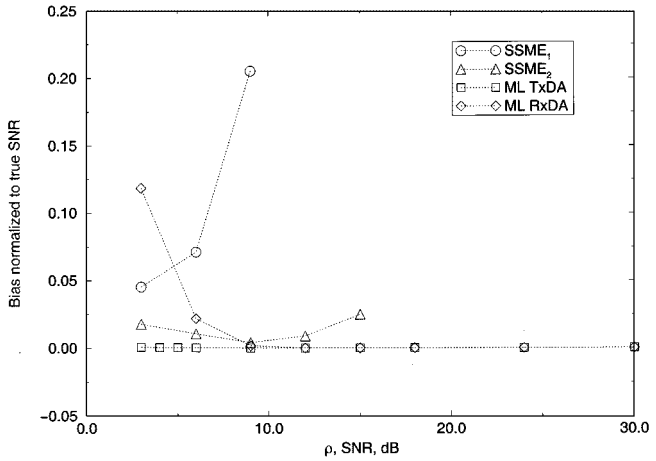

Fig. 3. Normalized bias with BPSK signals in real AWGN ($N_{\mathrm{ss}} = 16$ and $N_{\mathrm{sym}} = 1024$).

Immediately apparent is the fact that the NMSE curves of the ML TxDA SNR estimator are practically indistinguishable from the corresponding CRB's, and the RxDA counterpart performs equally well as long as the SNR is high enough to avoid excessive receiver errors. The performance difference between the ML TxDA and ML RxDA estimators decreases with decreasing block length as the effect of the inherent variance of the ML RxDA estimator on the MSE becomes comparable to the effect of the bias caused by receiver errors. Despite the appearance, on first inspection, that the ML TxDA estimator is efficient, its variance is slightly worse than the CRB which, graphically, can be seen only when the sample size is very small. Thomas [12] has shown analytically for the case of BPSK-modulated signals in AWGN that the ML TxDA SNR estimator is not efficient so there may exist another estimator whose performance comes even closer to the CRB [9]; however, it can be seen from Figs. 2

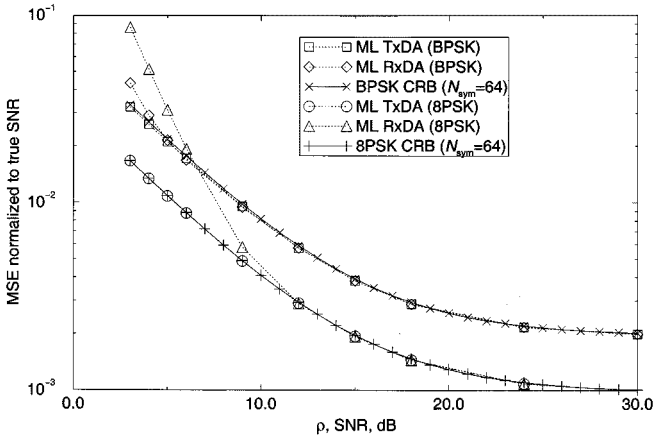

Fig. 4. Normalized MSE with BPSK and 8-PSK signals in AWGN ($N_{\rm ss} = 16$ and $N_{\rm sym} = 64$).

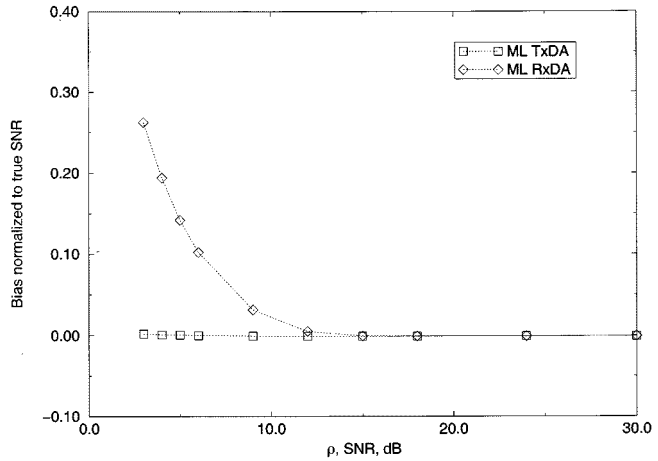

Fig. 5. Normalized bias with 8-PSK signals in complex AWGN ($N_{\rm ss} = 16$ and $N_{\rm sym} = 64$).

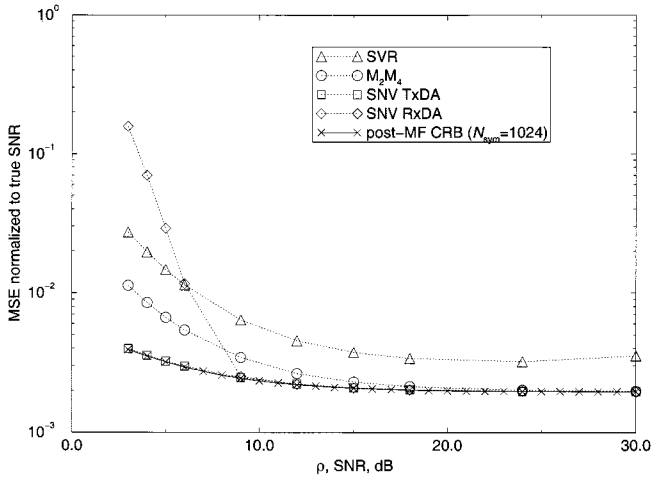

Fig. 6. Normalized MSE with BPSK signals in real AWGN ($N_{\rm ss} = 1$ and $N_{\rm sym} = 1024$).

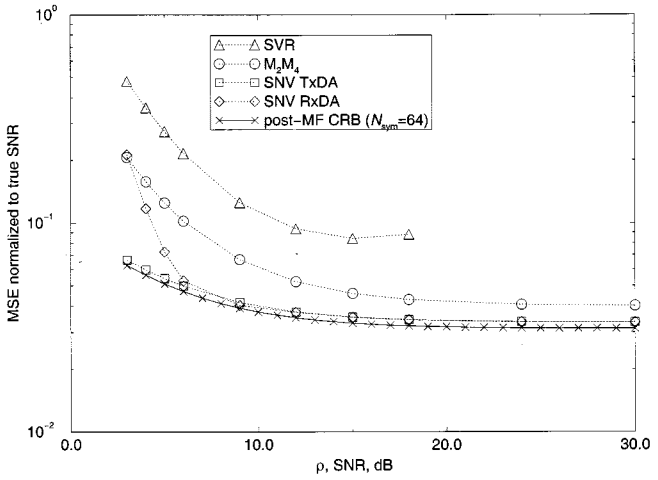

Fig. 7. Normalized MSE with BPSK signals in real AWGN ($N_{\rm ss} = 1$ and $N_{\rm sym} = 64$).

and 4 that there is little practical merit to motivate a search for such an estimator.

The SSME_1 and SSME_2 do not generally perform as well as the ML TxDA and ML RxDA estimators, though the modified approach that led to the SSME_2 yields a slightly better estimator than the SSME_1 as is evident in both Figs. 2 and 3. For low SNR (less than about 9 dB), the bias of the SSME_2 is smaller than that of the ML RxDA, but its NMSE is worse for the entire tested range of SNR. Interestingly, the NMSE and the bias increase with increasing SNR. This behavior is described more fully in the sequel. We have observed that some estimators based on higher-order moments converge poorly in band-limited channels. The SSME_1 and SSME_2 are examples. We have tried applying these estimators at the input to the MF rather than the output, and have observed similar results.

For comparison, Figs. 4 and 5 show the NMSE and bias plots, respectively, of the ML TxDA and ML RxDA estimators for 8-PSK-modulated signals in a complex AWGN channel using a block length of $N_{\rm sym} = 64$ symbols. The SSME_1 and SSME_2 are not included since these estimators are designed for BPSK-modulated signals and are not easily extended to higher orders of modulation. In Fig. 4, comparing the BPSK results to the 8-PSK results, the NMSE curves are a factor of two better in the 8-PSK case, which is consistent with the CRB results of (65) and (67). However, the performance of the ML RxDA estimator with 8-PSK signals is inferior to its performance with BPSK signals at low SNR since receiver errors are more likely in the 8-PSK case given equal signal and noise powers.

Figs. 6–10 compare those estimators that operate on the one ISI-free sample per symbol at the output of the MF. Figs. 6–8 compare the performances of the SVR, M_2M_4, SNV TxDA, and SNV RxDA SNR estimators for BPSK-modulated signals in a real AWGN channel. In Fig. 6, $N_{\rm sym} = 1024$ symbols, and results for $N_{\rm sym} = 64$ symbols are provided in Fig. 7. Accompanying Fig. 7, Fig. 8 shows the estimator biases using a block length of 64 symbols. Finally, Figs. 9 and 10 show the NMSE and bias plots, respectively, of the SVR, M_2M_4, SNV TxDA, and SNV RxDA SNR estimators for 8-PSK-modulated signals in complex AWGN using a block length of 64 symbols.

The performances of the SNV estimators parallel those of the ML estimators in every respect. The SNV TxDA estimator is asymptotically efficient (in Fig. 7, the number of samples is small enough to see that the SNV TxDA estimator is not efficient). The SNV RxDA estimator is asymptotically efficient

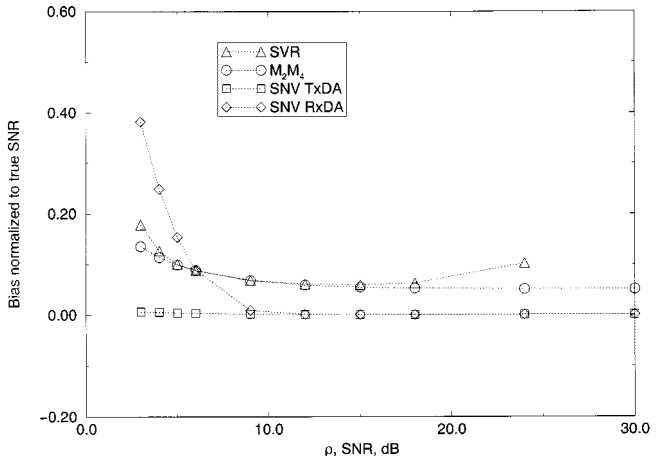

Fig. 8. Normalized bias with BPSK signals in real AWGN ($N_{\rm ss} = 1$ and $N_{\rm sym} = 64$).

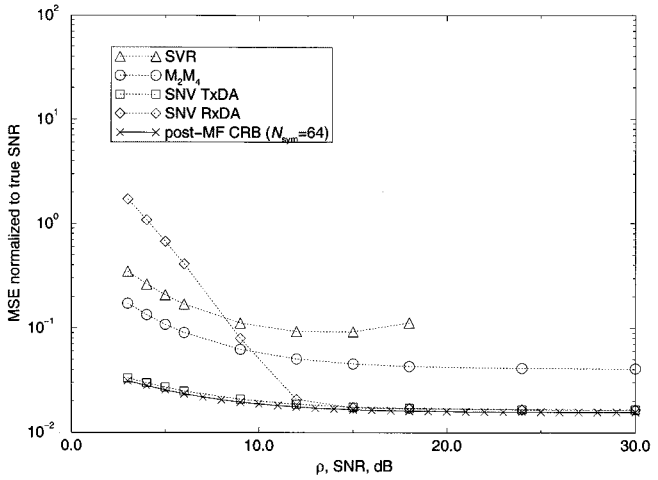

Fig. 9. Normalized MSE with 8-PSK signals in complex AWGN ($N_{\rm ss} = 1$ and $N_{\rm sym} = 64$).

at high SNR. The performance difference between the SNV RxDA and SNV TxDA estimators decreases with decreasing block length. The NMSE curves of the SNV RxDA (at high SNR) and SNV TxDA estimators are a factor of two better in the 8-PSK case as compared to the BPSK case. Finally, the performance of the SNV RxDA estimator with 8-PSK signals is inferior to its performance with BPSK signals at low SNR since, as already mentioned, receiver errors are more likely in the 8-PSK case given equal signal and noise powers.

The M_2M_4 estimator is asymptotically efficient at high SNR. Its performance at low SNR becomes relatively better than that of the SNV RxDA estimator as the block length increases, and as the number of signal constellation points M increases. Interestingly, the NMSE of the M_2M_4 estimator is close to identical in real and complex channels, in contrast to the CRB and the NMSE of the SNV TxDA estimator (and the NMSE of the SNV RxDA estimator at high SNR) which are a factor of two smaller in complex channels.

The SVR estimator does not generally perform as well as the M_2M_4, SNV TxDA, and SNV RxDA estimators though, in some cases, it has an advantage over the SNV RxDA estimator at low SNR. The SVR estimator is another example of a method

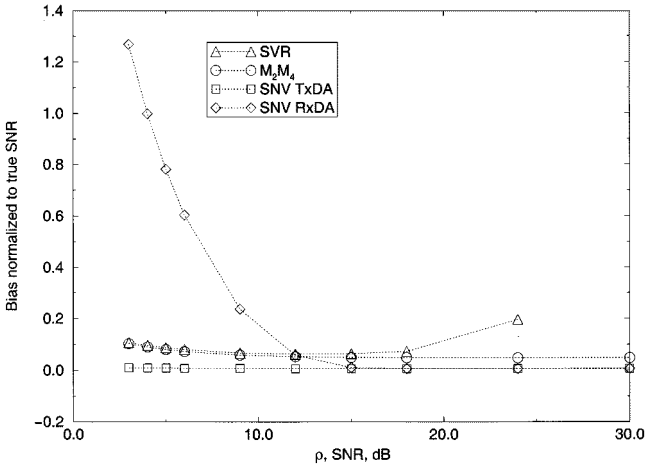

Fig. 10. Normalized bias with 8-PSK signals in complex AWGN ($N_{\rm ss} = 1$ and $N_{\rm sym} = 64$).

based on higher-order moments that has an NMSE and a bias that begin to increase after the SNR is increased beyond a certain threshold. The effect is more pronounced with smaller block sizes. The degradation in performance for values of SNR greater than about 20 dB with $N_{\rm sym} = 64$ is so severe that the estimates are meaningless (which is the reason why some high-SNR points are omitted from the SVR curves in Figs. 7–10).

Though the exact mechanism that causes the NMSE to increase at high SNR is not fully understood, it is not unreasonable that this effect should occur. Note that the CRB itself, normalized to the true SNR, does not decrease indefinitely with increasing SNR but, instead, approaches a constant. Since the performances of the *10pbest* estimators cannot be better than the CRB, the NMSE's of those estimators, at best, also approach a constant at high SNR. Consequently, it is not unreasonable to expect the NMSE of an inferior estimator either to approach some larger constant or to increase with increasing SNR. Generally, estimators or computations that are based on higher-order moments may be problematic at larger values of SNR; for example, moment-based methods for ISI error-rate calculations have such problems [19]. We have observed that this phenomenon is common among estimators based on higher-order moments, though there are exceptions. For example, though the M_2M_4 estimator is based on higher-order moments, its NMSE and bias plots are "well behaved;" that is, the curves asymptotically approach constant values at high SNR.

V. Conclusions

The "best" estimator to use depends on the given application. If known data is available at the receiver, the ML TxDA and SNV TxDA estimators perform so well as to invalidate attempts to find better estimators for the channel conditions considered here. Of course, these estimators can only generate SNR estimates at those times that known data is transmitted which may or may not be an objectionable limitation, depending on the application. If uninterrupted SNR estimates are required for an application, then one of the in-service SNR estimators would be more appropriate. The "best" in-service estimator to use depends on the block length, the number of samples per symbol

available, the type of modulation used, and the SNR range of interest. Complexity is also a factor to consider. Fortunately, the estimators that we have found to perform best (the ML, SNV, and M_2M_4 estimators) are also relatively easy to implement. As an example, a hardware implementation of the M_2M_4 estimator is described in [18].

The performances we have reported here of the SVR, M_2M_4, and SNV estimators are identical among systems that employ any type of root-Nyquist filter (not necessarily an RRC filter) in the transmitter and receiver, as long as the sum of the squares of the filter coefficients is unity. The performances of the ML estimators are identical even in systems for which Nyquist's criterion for ISI-free transmission is not satisfied, as long as the sum of the squares of the filter coefficients in the transmitter is unity. The performances of the SSME_1 and SSME_2 estimators are channel-dependent, and the results reported here are specific to the real form of the channel model described in Section II.

ACKNOWLEDGMENT

The authors would like to thank R. Matzner of the Federal Armed Forces University Munich, Neubiberg, Germany, and B. Shah of the Jet Propulsion Laboratory, Pasadena, CA, for their cooperation and for sharing their resources on this topic. The authors would also like to thank the anonymous reviewers whose comments led to improvements to the discussion and results.

REFERENCES

[1] D. G. Brennan, "Linear diversity combining techniques," *Proc. IRE*, vol. 47, pp. 1075–1102, June 1959.
[2] J. Hagenauer and P. Hoeher, "A Viterbi algorithm with soft-decision outputs and its applications," in *Proc. IEEE Global Telecommunications Conf.*, Dallas, TX, Nov. 1989, pp. 1680–1686.
[3] P. A. Wintz and E. J. Luecke, "Performance of optimum and suboptimum synchronizers," *IEEE Trans. Commun.*, vol. COM-17, pp. 380–389, June 1969.
[4] E. A. Newcombe and S. Pasupathy, "Error rate monitoring for digital communications," *Proc. IEEE*, vol. 70, pp. 805–828, Aug. 1982.
[5] M. K. Simon and A. Mileant, "SNR estimation for the baseband assembly," Jet Propulsion Lab., Pasadena, CA, Telecommunications and Data Acquisition Prog. Rep. 42-85, May 15, 1986.
[6] B. Shah and S. Hinedi, "The split symbol moments SNR estimator in narrow-band channels," *IEEE Trans. Aerosp. Electron. Syst.*, vol. AES-26, pp. 737–747, Sept. 1990.
[7] B. Shah and J. K. Holmes, "Improving the Split-Symbol Moments SNR Estimator," Jet Propulsion Lab., Pasadena, CA, Interoffice Memo. 3338-90-223, Dec. 19, 1990.
[8] D. R. Pauluzzi, "Signal-to-Noise Ratio and Signal-to-Impairment Ratio Estimation in AWGN and Wireless Channels," M. Sc. (Eng.) thesis, Queen's Univ., Kingston, ON, Canada, 1997.
[9] H. L. Van Trees, *Detection, Estimation, and Modulation Theory*. New York: Wiley, 1968, vol. 1.
[10] R. B. Kerr, "On signal and noise level estimation in a coherent PCM channel," *IEEE Trans. Aerosp. Electron. Syst.*, vol. AES-2, pp. 450–454, July 1966.
[11] R. M. Gagliardi and C. M. Thomas, "PCM data reliability monitoring through estimation of signal-to-noise ratio," *IEEE Trans. Commun.*, vol. COM-16, pp. 479–486, June 1968.
[12] C. M. Thomas, "Maximum Likelihood Estimation of Signal-to-Noise Ratio," Ph.D. dissertation, Univ. of Southern California, Los Angeles, 1967.
[13] C. E. Gilchriest, "Signal-to-noise monitoring," *JPL Space Programs Summary*, vol. IV, no. 37-27, pp. 169–184, June 1966.
[14] T. R. Benedict and T. T. Soong, "The joint estimation of signal and noise from the sum envelope," *IEEE Trans. Inform. Theory*, vol. IT-13, pp. 447–454, July 1967.
[15] R. Matzner, "An SNR estimation algorithm for complex baseband signals using higher order statistics," *Facta Universitatis (Nis)*, no. 6, pp. 41–52, 1993.
[16] R. Matzner and F. Engleberger, "An SNR estimation algorithm using fourth-order moments," in *Proc. IEEE Int. Symp. Information Theory*, Trondheim, Norway, June 1994, p. 119.
[17] A. L. Brandão, L. B. Lopes, and D. C. McLernon, "In-service monitoring of multipath delay and cochannel interference for indoor mobile communication systems," *Proc. IEEE Int. Conf. Communications*, vol. 3, pp. 1458–1462, May 1994.
[18] R. Matzner, F. Engleberger, and R. Siewert, "Analysis and design of a blind statistical SNR estimator," in *AES 102nd Convention*, München, Germany, Mar. 1997.
[19] K. Metzger, "On the probability density of intersymbol interference," *IEEE Trans. Commun.*, vol. COM-35, pp. 396–402, Apr. 1987.

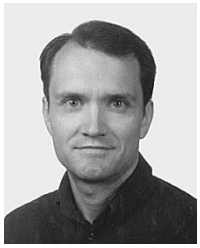

David R. Pauluzzi was born in Penticton, BC, Canada, in 1966. He received the B.A.Sc. degree in engineering physics from the University of British Columbia, Vancouver, BC, Canada, in 1989, and the M.Sc. degree in electrical engineering from Queen's University, Kingston, ON, Canada, in 1997.

For four years, he was with MPR Teltech, Burnaby, Canada, where he worked on the physical layer DSP and FPGA implementation of radio and infrared systems. Since 1997, he has been with DATUM Telegraphic, Inc. (now the Wireless Products Division of PMC-Sierra, Inc.), Vancouver, BC, Canada, as a Consultant to companies involved in the development of wireless data systems. His current projects include the modeling and specification of modulation, coding, and equalization schemes and transmit/receive architectures for ISM-band mobile wireless internet devices.

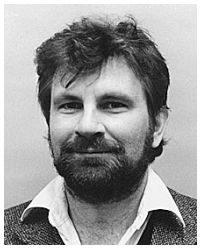

Norman C. Beaulieu (S'82–M'86–SM'89–F'99) received the B.A.Sc. (honors), M.A.Sc., and Ph.D. degrees in electrical engineering in 1980, 1983, and 1986, respectively, from the University of British Columbia, Vancouver, BC, Canada. In 1980, he was awarded the University of British Columbia Special University Prize in Applied Science.

He held an appointment as Queen's National Scholar Assistant Professor in the Department of Electrical Engineering at Queen's University, Kingston, ON, Canada, from September 1986 to June 1988. From July 1988 to June 1993, he held the position of Associate Professor. Since July 1993, he has been a Professor of Electrical Engineering at Queen's. His current research interests include digital communications over fading channels, interference effects in digital modulations, channel modeling and simulation, decision-feedback equalization, and digital synchronization in sampled receivers.

Dr. Beaulieu is a member of the Communication Theory Committee. He served as representative of the Communication Theory Committee to the Technical Program Committee of the 1991 International Conference on Communications and as co-representative of the Communication Theory Committee to the Technical Program Committee of the 1993 International Conference on Communications and the 1996 International Conference on Communications. He was General Chair of the Sixth Communication Theory Mini-Conference in association with GLOBECOM'97, and Co-Chair of the Canadian Workshop on Information Theory 1999. Since January 1992, he has served as Editor for Wireless Communication Theory of the IEEE TRANSACTIONS ON COMMUNICATIONS. Since November 1996, he has served as Associate Editor for Wireless Communication Theory of the IEEE COMMUNICATIONS LETTERS. Effective January 2000, Dr. Beaulieu was appointed Editor-in-Chief of the IEEE TRANSACTIONS ON COMMUNICATIONS. He was a recipient of the Natural Science and Engineering Research Council (NSERC) E.WR. Steacie Memorial Fellowship in 1999.